



## GREEN SYNTHETIC STRATEGIES OF OXIDE MATERIALS: POLYSACCHARIDES-ASSISTED SYNTHESIS. PART IV. ALGINATE-ASSISTED SYNTHESIS OF NANOSIZED METAL OXIDES

Oana CARP,<sup>a\*</sup> Diana VISINESCU,<sup>a</sup> Greta PATRINOIU<sup>a</sup> and Alina TIRSOAGA<sup>b</sup>

<sup>a</sup>Institute of Physical Chemistry "Ilie Murgulescu", Coordination and Supramolecular Chemistry Laboratory,  
202 Splaiul Independenței, 060021 Bucharest, Roumania

<sup>b</sup>University of Bucharest, Faculty of Chemistry Physical Chemistry Department, 4-12 Bd. Elisabeta, 030018 Bucharest, Roumania

Received May 20, 2011

The possibilities of using alginate as an efficient raw material in the oxide synthesis of oxide materials are analyzed in the present paper. The main developed synthetic routes are reviewed, with a special emphasis on the gel-template ones, strategies that exploit the alginate particular gel formation mechanism.

### INTRODUCTION

Alginic acid is a natural polymer produced from brown marine algae (*Phaeophyceae*) widely found over the planet's coasts, and by soil bacteria (*Azotobacter vinelandii* and *Pseudomonas* species).<sup>1,2</sup> Discovered by Edward Stanford in 1883, its commercial production started in 1927. Used initially only as thickening agent, both in food and in the textile industries, applications still valid due to alginates ability to retain water and gel-forming, viscosifying and stabilizing properties,<sup>3</sup> nowadays polysaccharide's uses in biotechnological and biomedical fields<sup>4</sup> such as bio-labeling,<sup>5,6</sup> cell culturing,<sup>7</sup> encapsulation of cells for transplantation<sup>8</sup> and heat-triggered drug release<sup>9,10</sup> have expanded.

Chemically, the anionic polysaccharides alginates are linear block copolymers composed of 1,4-linked  $\beta$ -D-mannuronic acid (M) and  $\alpha$ -L-guluronic acid (G), both in the pyranosic conformation, arranged in a nonregular blockwise pattern by varying proportions of GG, MG, and MM blocks (Fig. 1).<sup>11-17</sup> This primary structure is generally defined by the  $F_G$  value, which is the fraction of overall guluronic acid residues in the

polymer, and by  $N_G$ , the average number of guluronic units in G-blocks. The amount, the sequential distribution of GG, MG, and MM blocks and implicit the alginates physical and chemical properties depend on the producing species, and for marine sources, on seasonal and geographical variations.<sup>18-20</sup>

In solid state, X-ray analysis of extended fibers suggested a helical conformation for the different types of blocks:<sup>21-23</sup> a two-fold helix for the mannuronic block, a three-fold helix for guluronic blocks when present as sodium salt and, a two-fold helix for the guluronic block in the presence of calcium salt.

The alginates are known to form gels either by hydrogen bonding at low pH (acid gel), or by ionic interactions with divalent ( $\text{Ca}^{2+}$ ,  $\text{Sr}^{2+}$ , and  $\text{Ba}^{2+}$  but not  $\text{Mg}^{2+}$ ) and trivalent ( $\text{Fe}^{3+}$  and  $\text{Al}^{3+}$ ) cations.<sup>24-28</sup> In the first case the homopolymeric blocks form the junctions and the gels stability is determined by the relative content and length of the G-blocks.<sup>29</sup> In the second case, the cations act as crosslinkers between two adjacent polymer chains (Fig. 2), the poly-G blocks being mainly responsible of such ionic interactions, as in the presence of multivalent

\* Corresponding author: [carp@acodarom.ro](mailto:carp@acodarom.ro)

cations they can associate to form aggregates of the “egg-box” model of ion binding. The term “egg box” arises from the similitude between the arrangement of the cations into electronegative cavities and eggs in an egg-box.<sup>24,25,26,28,30,31</sup> Within the “egg-box” domains, the divalent/trivalent cations forms intermolecular bonds *via* two hydroxyl groups of one G-chain and two deprotonated carboxylate groups of another chain.<sup>32-34</sup>

An alginate with a higher level of G sequences presents a higher affinity for cross-linking agents than low G-containing alginates.<sup>35</sup> The selective binding of divalent/trivalent metal ions and the corresponding gel strength were found to increase in the order: MM block < MG block < GG block.<sup>36</sup> It

has been reported that alginates with a high G blocks content (blocks in which axial-axial linkage is involved) develop a stiffer, more brittle, and more porous gel, which maintains its integrity for long periods of time. Also it has been found that the greater the G content of the gel, the greater is the restriction to solute transport.<sup>37</sup> Equally, alginates rich in M residues (diequatorially linked) undergoes a high degree of swelling during cations crosslinking<sup>25</sup>, developing softer and less porous beads, which tend to disintegrate easier with time. Besides the alginate compositions, the properties of the metallic containing gel depend on cation nature and concentration and, reaction experimental conditions, specially the pH.<sup>38-40</sup>

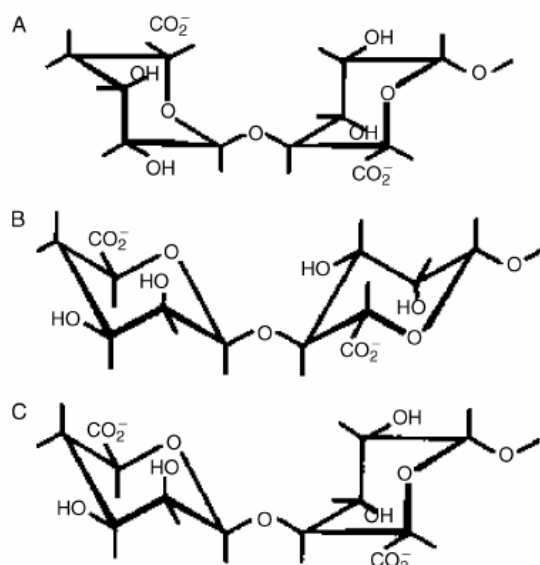


Fig. 1 – Chemical structure of repeat units of alginates: (A) L-guluronic acid (G); (B) D-mannuronic acid (M); (C) alternating L-guluronic and D-mannuronic acids (GM).

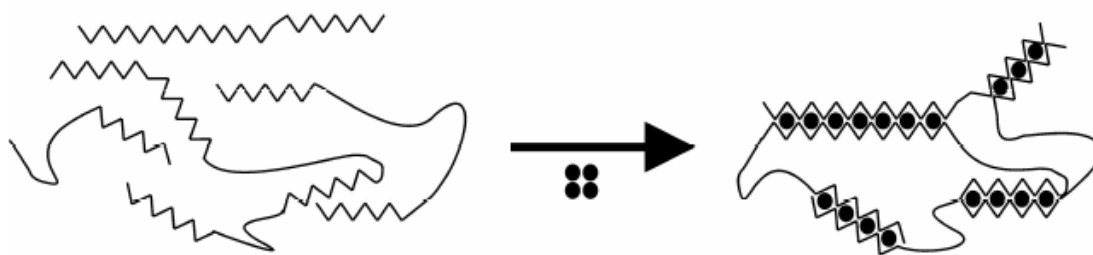


Fig. 2 – The “egg box” ion binding model in alginate gel between G-block alginate and divalent/trivalent cations (●).

Gels with a uniform concentration of alginate can be obtained by cross-linking *via* the internal setting method,<sup>31,41</sup> a technique that allows a controlled gelation of alginate through a slow release of the cations, leading thus to the formation of a very regular gel network. The gel can be easily converted into a solution by adding sodium, magnesium (non-gelling ions) or complexants for the metallic cations (such as and EDTA).

#### ALGINATE-ASSISTED GEL-TEMPLATE METHODS OF OXIDES SYNTHESIS

It is obvious that the very particular gel formation process that involves the development of ordered domains in which the polymer chain network defines a confined space for cation localization, represents a useful feature which can be exploited for the controlled growth of cationic

species. As demonstrated for iron oxide nanoparticles formed by magnetotactic bacteria,<sup>42</sup> such a confinement is a key feature in numerous biomineralization processes, playing a major role in the nucleation and growth controlling.

The decompositions of the investigated bivalent cations alginate gels (M(II)=Co, Cu, Pb, Cd, Sr, Hg and Ni) is two-stepped, starting at temperatures of  $\sim 150^\circ\text{C}$  and ending at  $\sim 500^\circ\text{C}$ .<sup>32,43</sup> A close temperature is registered for titanium containing gels also.<sup>44</sup> Oxalate intermediates are identified for Pb-, Cd-gels while for Sr-, Hg-ones, carbonate intermediates were detected.<sup>32</sup>

ZnO nanocrystals were obtained by the thermal decomposition of zinc alginate beads.<sup>45</sup> The mean particle size is influenced by the zinc (II) raw material: the use of zinc nitrate determines the formation of smaller crystals (50 nm) with more uniform distribution than zinc acetate (125 nm), differences attributed to the distinct binding capacities of alginates to the zinc species (zinc acetate or zinc nitrate).

$\text{Y}_2\text{O}_3$  microparticles, (500  $\mu\text{m}$ ) with pores of less 1  $\mu\text{m}$  in diameter and low density ( $0.66 \text{ g m}^{-3}$ ) can be obtained by calcinations at  $1100^\circ\text{C}$  of  $\text{Y}^{3+}$ -alginate gel. The chemical durability of the porous  $\text{Y}_2\text{O}_3$  microparticles was estimated to be high enough for clinical application as *in situ* radiotherapy of cancer.<sup>46</sup>

Monodisperse iron non magnetic oxides,  $\alpha\text{-Fe}_2\text{O}_3$  were obtained from alginate gels, after a heating treatment at  $700^\circ\text{C}$ .<sup>47,48</sup> An acidic pH (3.5) favored the monodisperse character and lower particle sizes, because at higher pH values the iron cations are converted to iron hydroxide prior to their interaction with alginate.

Nanocrystals of CuO,  $\text{Co}_3\text{O}_4$  and NiO oxides aggregated in hollow millimetric spheres shape were obtained after a calcinations treatment at  $500^\circ\text{C}$  of the M(II)-alginate aerogels.<sup>49</sup> The oxide preserves the spherical shape of the parent aerogel, but the size of the calcined spheres is nearly one third of the original size.

Using the gel-template method, and sodium alginate as gelling agent, single-phase well-tiled flaky agglomerations could be obtained with the assembly of flaky  $\gamma\text{-Na}_x\text{Co}_2\text{O}_4$  single crystals along the plane direction.<sup>50</sup> Sodium alginate not only controlled the arrangement of crystals, but also provided sodium for the  $\gamma\text{-Na}_x\text{Co}_2\text{O}_4$  crystals.

Single-crystal nanowires complex oxides such as yttrium–barium–copper-oxide (YBCO) superconductor<sup>51</sup> and lanthanum-strontium-manganese (LSMO) perovskite<sup>52</sup> were also

obtained using alginate as template. For both mixed oxides fascinating mechanisms were determined. In the case of YBCO the cocooning effect of the alginate biopolymer due to the alginate egg-box binding model prevented the coalescence of the barium nanoparticles, leading to uniform, homogeneously dispersed nanoparticles throughout the matrix, which were able subsequently, to act as preferential sites of nucleation for barium carbonate nanoparticles. On calcination, the growth of superconductor needles occurred radially from partially embedded barium carbonate nanoparticles exposed on the surface of the amorphous material. The material is made up from a complex microstructure of fibrous aggregates, up to several micrometres in thickness (Fig. 3a), with smooth surfaces and a circular cross section of 50–80 nm in diameter (Fig. 3b). Each fiber includes bundles of straight-sided nanowires, typically with 10 nm in diameter (Fig. 3c). The fibres were uniaxially aligned, with a preferred direction of growth (Fig. 3d), while the constituted nanowires have a critical temperature of 77 K, which is only slightly lower than the one, specific for YBCO (85–89 K).

A molten-salt mechanism is ascertained for LSMO synthesis, starting from a sodium alginate gel that contains the corresponding cations. During the decomposition processes  $\text{Na}_2\text{CO}_3$  is formed. At approximately  $850^\circ\text{C}$  it melts, facilitating the transformation of  $\text{LaMnO}_3$  to the Sr-doped manganite product by dissolving or dispersing one or more of the intermediate precursors and aiding transport of the reactants.

Although, as mentioned before, it is known that the structure and properties of alginate gels varies widely, both on alginate composition and reaction experimental conditions, no systematic investigations gel properties-oxides characteristics is till now performed.

### ALGINATE-ASSISTED (CO) PRECIPITATION METHODS OF OXIDES SYNTHESIS

Recently, numerous investigations dealing with the precipitation of magnetically iron oxide nanoparticles in alginate presence were performed<sup>53-57</sup>, being developed several synthesis strategies: (A) *in situ* synthesis coating starting from ferrous salts; (B) *post* synthesis coating starting from ferrous/feric salts; (C) *post* synthesis coating starting from ferric salts.

The standard *in situ* chemical synthesis coating (A) of iron oxide in fibrillar suspensions or gels of alginate (A) consists in three steps: (a) ferrous ion-absorption by the original polymer materials following polymer swelling or gelation into a ferrous salt solution; (b) *in situ* precipitation of ferrous hydroxide by an alkaline treatment of swollen alginate, usually with aqueous sodium hydroxide; (c) oxidation of ferrous hydroxide with an oxidizing agent, such as  $O_2$  or  $H_2O_2$ .

The method is complex because involves multiple recycles<sup>53,54,56,57</sup> to produce composites with an iron oxide content about 50%, needing also a control of the complicated oxidation reaction in order to avoid the production of nonmagnetic forms of iron oxide (such as  $FeOOH$ ).<sup>28</sup> The iron oxide prepared by the three-stepped method is usually  $\gamma-Fe_2O_3$  being characterized by a lower saturation magnetization comparative with  $Fe_3O_4$ . Additionally, an aggregation of the iron oxide may also occur, due to the conformational restrictions of the alginate polymeric backbone.<sup>58</sup>

The post synthesis alginate coating (B) involves two stages, leading mainly to  $Fe_3O_4$  in a higher content compared with the first *in situ* method: (a) formation of  $Fe_3O_4$  by coprecipitation of ferric and

ferrous ion with an alkaline solution; (b) binding of alginate polymer to iron oxide.

Using a method of this type,  $Fe_3O_4$  characterized by a saturation magnetization of 55 emu/g with a core diameter of 5-10 nm and an oxide-alginate composite with a hydrodynamic diameter of 193.8-483.2 nm are obtained.<sup>59</sup> Magnetite alginates beads prepared by this simple post synthesis method were used with success to purify starch degrading enzymes ( $\beta$ -amylase, glucoamylase and pullulanase).<sup>60</sup>

The *post* synthesis coating starting from ferric salts (C) exploits the alginate mild reducing properties on heating. Such properties arised from its high hydroxyl content, the C-OH groups being oxidized at the temperature rising into carboxyl ones simultaneously with the reduction of metallic cations  $M^{n+} \rightarrow M^{m+}/M^0$  (where  $n>m$ ).<sup>61</sup> This ability of alginate to form a gel with metal ions that can be further reduced was already exploited in the synthesis of gold nanodisks.<sup>61,62</sup> Starting from ferric salts, magnetite with a saturation magnetization value about 62.1 emu/g<sup>63</sup> was obtained. Without the addition of sodium alginate, the final products are pure  $\alpha-Fe_2O_3$ , even when other experimental conditions are kept the same.<sup>63</sup>

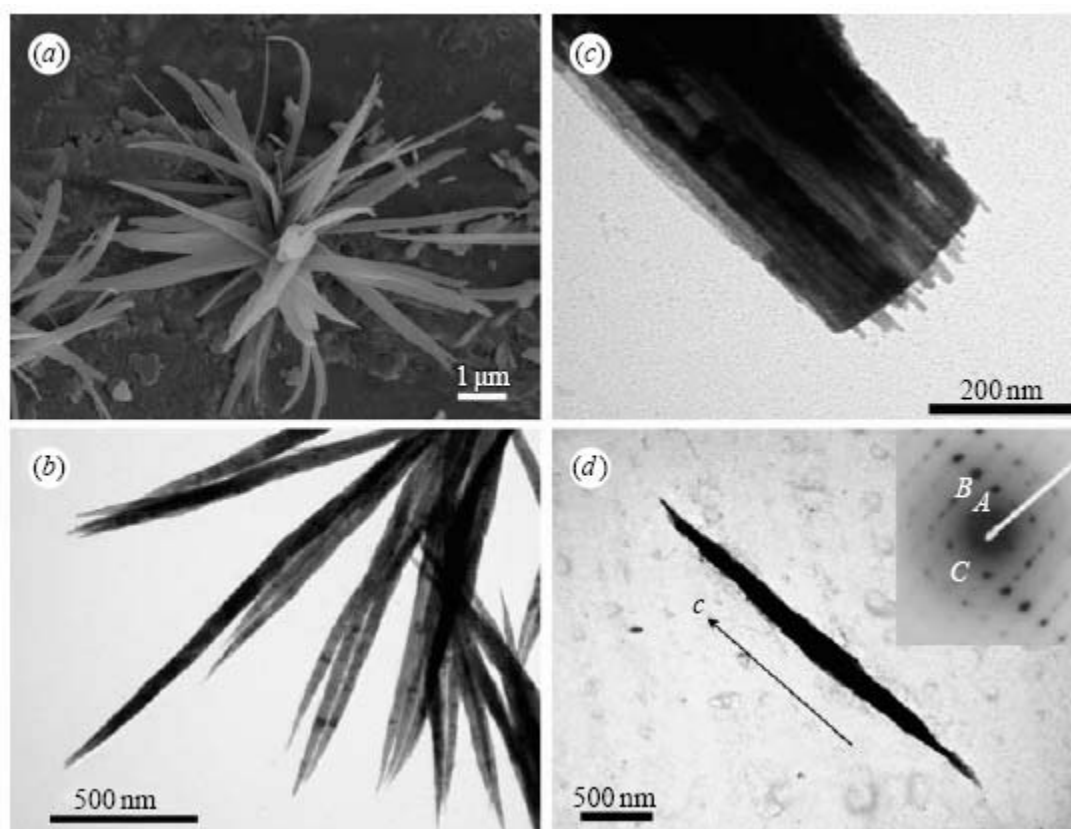


Fig. 3 – (a) SEM image, (b–d) TEM images and corresponding single crystal electron diffraction pattern (d inset) of YBCO nanowires.<sup>51</sup>

## ALGINATE-ASSISTED HYDROTHERMAL METHODS OF OXIDES SYNTHESIS

Several interesting three-dimensional (3-D) ZnO architectures – microspheres and other radial structures were obtained using alginate as soft template.<sup>64</sup> The strategies rely on the one-dimensional ZnO nanorods self-assembly into hierarchical structures obtained using hydrothermal procedures at low temperatures of 100°C and normal<sup>65</sup> or autogenous pressures.<sup>64,65</sup> The water-soluble long-chain biopolymer constitutes the nucleation site for the self-assembly of radial structures, offering the possibility to control growth process for 3-D architectures.

Two critical factors influence the self-assembly process of the hollow microspheres: the water-soluble alginate amount and pH value of solution (Fig. 4). In basic media (pH = 10.38) and in the absence of the polysaccharide, no internal hole is formed, the ZnO nanorods being rooted in one center and radially extended outward (Fig. 4A). In the presence of a certain amount of sodium alginate, the ZnO nanorods have built spherical architectures (Fig. 4B), while a five times dosage of polysaccharide has led to a different type of hierarchical superstructures, namely the hemispheric structures (Fig. 4C). When the pH value was decreased to 9.96, the product has a flower-shaped structure (Fig. 4D) while for a value of 10.48 or higher, the structure has become nonuniform in terms of morphology and size (Fig. 4E).

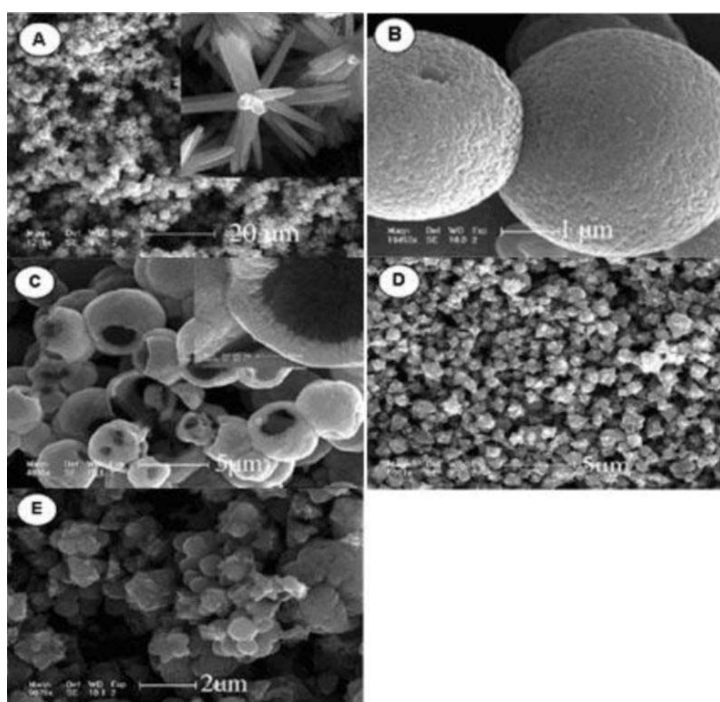


Fig. 4 – Field emission scanning electron microscopy (FESEM) images of samples obtained from control experiments: (A) in the absence of SA; (B) in the presence of SA under other identical conditions; (C) 5 times the dosage of SA under other identical conditions; (D) decreasing the pH value from 10.38 to 9.96; (E) and increasing the pH value from 10.38 to 10.48.<sup>64</sup>

## CONCLUSIONS

Till now, alginates chemistry was vigorously investigated mainly in connection with their biological, biomedical and food area applications. Comparatively with these researches, the ones which explore their use in materials synthesis, particularly in oxides ones are scarce, the present paper analyzing almost exhaustively the use of alginate in materials synthesis, in particular oxidic ones, highlighting the most important results and the significant benefits over existing technologies.

A general conclusion may be pointed out: the alginate assisted synthesis of materials, fulfills the

major desiderates of modern material science, the synthetic routes being versatile, predictable, less expensive and environmentally friendly, the obtained oxide-based materials presenting applications of interest and perspective.

## REFERENCES

1. G. Skjak-Braek, H. Grasdalen, B. Larsen, *Carbohydr. Res.*, **1986**, *154*, 239-250.
2. F. A. Johnson, D. Q. M. Craig, A. D. Mercer, *J. Pharm. Pharmacol.*, **1997**, *49*, 639-643.
3. O. Smidsrod and K. I. Draget, *Carbohydr. Eur.*, **1996**, *14*, 6-13.

4. (a) K. I. Draget, G. Skjak-Braek, O. Smidsrod, *Int. J. Biol. Macromol.*, **1997**, *21*, 47-55; (b) J. N. Barbotin, J. E. Nava Saucedo, in "Polysaccharide: Structural Diversity and Functional Versatility", Ed. S. Dimitriu, Marcel Dekker, New York, 1996, p. 125.
5. M. Fleischmann, P. J. Hendra, A. J. Maquillan, *Chem. Phys. Lett.*, **1974**, *26*, 163-166.
6. K. Kneipp, H. Kneipp, I. Itzkan, R. R. Dasari, M. S. Feld, *Chem. Rev.*, **1999**, *99*, 2957-2975.
7. J. A. Rowley, G. Madlambayan, D. J. Mooney, *Biomaterials*, **1999**, *20*, 45-53.
8. M. Machluf, A. Orsola, S. Boorjian, R. Kershen, A. Atala, *Endocrinology*, **2003**, *144*, 4975-4979.
9. U. O. Häfeli, *Int. J. Pharm.*, **2004**, *277*, 19-24.
10. S. Mornet, S. Vasseur, F. Grasset, E. Dugué, *J. Mater. Chem.*, **2004**, *14*, 2161-2175.
11. S. K. Chanda, E. L. Hirst, B. G. V. Percival, A. G. Ross, *J. Chem. Soc.*, **1952**, 1833-1837.
12. O. Smidsrod, A. Haug and B. Larsen, *Acta Chem. Scand.*, **1966**, *20*, 1026-1034.
13. B. Larsen, O. Smidsrod, A. Haug and T. Painter, *Acta Chem. Scand.*, **1969**, *23*, 2375-2388.
14. A. Haug, B. Larsen and O. Smidsrod, *Carbohydr. Res.*, **1974**, *32*, 217-225.
15. A. Haug, S. Myklestad, B. Larsen B and O. Smidsrod, *Acta Chem. Scand.*, **1967**, *21*, 768-788.
16. A. Haug, B. Larsen, O. Smidsod, *Acta Chem. Scand.*, **1966**, *20*, 183-190.
17. F. G. Fischer, H. Z. Dörfel, *Physiol. Chem.*, **1955**, *302*, 186-203.
18. O. Smidsrod, A. Haug, *Acta Chem. Scand.*, **1965**, *19*, 329-340.
19. O. Smidsrod, A. Haug, *Acta Chem Scand.*, **1965**, *19*, 341-354.
20. H. Zheng, *Carbohydr. Res.*, **1977**, *302*, 97-104.
21. E. D. T. Atkins, W. Mackie and E. E. Smolko, *Nature* **1970**, *225*, 626-628.
22. E. D. T. Atkins, D. H. Isaac, I. A. Nieduszynski and C. F. Phelps, *Polymer*, **1974**, *15*, 263-271.
23. E. D. T. Atkins, W. Mackie, K. D. Parker and E. E. Smolko, *J. Polym. Sci. Polym. Lett.*, **1971**, *9*, 311-316.
24. O. Smidsrod, A. Haug, *Acta Chem. Scand.* **1972**, *26*, 2063-2074.
25. G. T. Grant, E. R. Morris, D. A. Rees, P. J. C. Smith, D. Thom, *FEBS Lett.*, **1973**, *32*, 195-198.
26. M. V. Nesterova, S. A. Walton, J. Webb, *J. Inorg. Biochem.*, **2000**, *79*, 109-118.
27. P. V. Finotelli, M. A. Morales, M. H. Rocha-Leão, E. M. Baggio-Saitovitch, A. M. Rossi, *Mater. Sci. Eng. C*, **2004**, *24*, 625-629.
28. Y. Nishio, A. Yamada, K. Ezaki, Y. Miyashita, H. Furukawa, K. Horie, *Polymer*, **2004**, *45*, 7129-7136.
29. H. Grasdalen, B. Larsen and O. Smidsrod, *Carbohydr. Res.*, **1981**, *89*, 179-191.
30. K. I. Draget, O. Smidsrod, G. Skjak-Braek, in: "Polysaccharides II. Polysaccharides from eukaryotes, biopolymers", Vol. 6, E. J. Vandamme, S. De Baets, A. Steimbüchel, editors VCH Verlag: Wiley, **2002**. p. 215-244
31. D. K. Rassis, I. S. Saguy, A. Nussinovitch, *Food hydrocolloids*, **2002**, *16*, 139-151.
32. R. Brayner, T. Coradin, F. Fiévet-Vincent, J. Livage, F. Fiévet, *New. J. Chem.*, **2005**, *29*, 681-865.
33. R. M. Hassan, M. H. Wadan, A. Hassan, *Eur. Polym. J.*, **1988**, *24*, 281-283.
34. R. M. Hassan, A. M. Summan, M. K. Hassam, S. A. El-Shatoury, *Eur. Polym. J.*, **1989**, *25*, 1209-1212.
35. D. Serp, E. Cantana, C. Heinzen, U. V. Stockar, I. W. Marison, *Biotech. Bioeng.*, **2000**, *70*, 41-53.
36. O. Smidsrod, A. Haug, *Acta Chem. Scand.*, **1968**, *22*, 1989-1997.
37. B. Amsden, N. Turner, *Biotech. Bioeng.*, **1999**, *65*, 605-610.
38. J. E. Nava Saucedo, B. Audras, S. Jan, C. E. Bazinet, J. N. Barbotin, *FEBS Microbiol. Rev.*, **1994**, *14*, 93-98.
39. N. M. Velings, M. M. Mestdagh, *Polym. Gels Networks*, **1995**, *3*, 311-330.
40. S. Baskoutas, P. Giabouranis, S. N. Yannopoulos, V. Dracopoulos, L. Toth, A. Chrissanthopoulos, N. Bouropoulos, *Thin Solid Films*, **2007**, *515*, 8461-8464.
41. E. Onsoyen, in "Thickening and gelling agents for food" Imeson, A. (Ed.); Blackie Academic & Professional: London, 1992, p. 1-24.
42. E. Bauerlein, *Angew. Chem. Int. Ed.*, **2003**, *42*, 614-640.
43. K. S. Khairou, *J. Therm. Anal. Calorim.* **2002**, *69*, 583-588.
44. T. Sato, Y. Kaneko, *J. Ceram. Soc. Jpn., Int. ed.*, **1992**, *100*, 964.
45. S. Baskoutas, P. Giabouranis, S. N. Yannopoulos, V. Dracopoulos, L. Toth, A. Chrissanthopoulos, N. Bouropoulos, *Thin Solid Films*, **2007**, *515*, 8461-8464.
46. K. Masakazu, N. Matsui, Z. Li, T. Miyazaki, *J. Mater. Sci.: Mater. Med.*, **2010**, *21*, 1837-1843.
47. M. Nidhin, R. Indumathy, K. J. Sreeram and B. U. I. Nair, *Bull. Mater. Sci.*, **2008**, *31*, 93-96.
48. K. J. Sreeram, R. Indumathy, A. Rajaram, B. U. Nair, T. Ramasami, *Mater. Res. Bull.*, **2006**, *41*, 1875-1881.
49. R. Horga, F. Di Renzo, F. Quignard, *Applied Catal. A: Gen.*, **2007**, *325*, 251-255.
50. L. Zhang, X. Tang and W. Gao, *J. Electron. Mater.*, **2009**, *38*, 1229-1233.
51. Z. A. C Schnepf, S. C. Wimbush, S. Mann, S. R. Hall, *Adv. Mater.*, **2008**, *20*, 1782-1786.
52. Z. Schnepf, S. C. Wimbush, S. Mann, S. R. Hall, *CrystEngComm*, **2010**, *12*, 1410-1415.
53. Y. Nishio, A. Yamada, K. Ezaki, Y. Miyashita, H. Furukawa, K. Horie, *Polymer*, **2004**, *45*, 7129-7136.
54. F. Llanes, D. H. Ryan, R. H. Marchessault, *Int. J. Biol. Macromol.*, **2000**, *27*, 35-40.
55. P. V. Finotelli, M. A. Morales, M. H. Rocha-Leão, E. M. Baggio-Saitovitch, A. M. Rossi, *Mater. Sci. Eng.* **2004**, *24*, 625-629.
56. E. Kroll, F. M. Winnik, R. F. Ziolo, *Chem. Mater.*, **1996**, *8*, 1594-1596.
57. F. Shen, C. Poncet-Legrand, S. Somers, A. Slade, C. Yip, A. M. Duft, F. M. Winnik, P. L. Chang, *Biotechnol. Bioeng.*, **2003**, *83*, 282-292.
58. K. J. Sreeram, H. Yamini Shrivastava, B. U. Nair, *BBA-Gen Subj.*, **2004**, *1670*, 121-125.
59. H. L. Ma, X. R. Qi, Y. Maitani, T. Nagai, *Int. J. Pharma*, **2007**, *333*, 177-186.
60. S. Teotia, M. N. Gupta, *Mol. Biotechnol.*, **2002**, *20*, 231-237.
61. S. Gao, S. Zhang, K. Jiang, S. Yang, W. Lu, *Curr. Nanosci.*, **2008**, *4*, 145-150.
62. A. Pal, K. Esumi, T. Pal, *J. Colloid Interface Sci.*, **2005**, *288*, 396-401.
63. S. Gao, Y. Shi, S. Zhang, K. Jiang, S. Yang, Z. Li, and E. Takayama-Muromachi, *J. Phys. Chem. C* **2008**, *112*, 10398-10401.
64. S. Gao, H. Zhang, X. Wang, R. Deng, D. Sun, and G. Zheng, *J. Phys. Chem. B*, **2006**, *110*, 15847-15852.
65. O. Lupana, L. Chowb, G. Chaic, A. Schulteb, S. Parkb, O. Lopatiuk-Tirpakb, L. Chernyakb, H. Heinrich, *Superlattices and Microstructures*, **2008**, *43*, 292-302.